

# Precision Spindle Metrology

Eric R. Marsh

DEStech Publications, Lancaster, PA

in cooperation with  
Lion Precision, St. Paul, MN  
and  
Professional Instruments, Hopkins, MN

Indicates end of sample content. The next page will be out of sequence.

# Contents

Preface	v
1 Introduction	1
2 Spindle Metrology Concepts	15
3 Test Instrumentation	39
4 Data Analysis	59
5 Production Equipment Case Studies	105
6 Applications	127
Bibliography	147
Index	159
About the Author	161

# Preface

This book describes concepts and techniques to properly measure machine tool and instrument spindles. The results of these measurements are invaluable for identifying and correcting problems. When seeking to improve a precision instrument, reliable spindle measurements provide insight needed to achieve higher performance in both manufacturing and metrology.

We begin with an introduction to the fundamental issues of spindles and spindle metrology. Fortunately, a standardized framework for considering the many facets of spindle behavior is available in the ASME B89.3.4 Axis of Rotation standard. This document provides the vocabulary and defines the issues so that metrologists can share results and work together to advance the state of the art. The most significant contribution of B89.3.4 is its unambiguous definition of the properties of a spindle. With the Standard in hand, two metrologists in different labs will be able to negotiate the details of a spindle measurement or purchase order specification. The author enjoyed the privilege of serving on this committee during a significant updating of the original 1985 document and of working alongside many of the leading spindle experts in the United States.

The B89.3.4 Standard does not attempt to exhaustively describe the experimental procedures needed to accurately capture the error motion of a spindle; that is the goal of this book. As the methods for spindle testing are introduced, the reader will find that a spindle is inevitably an important part of a larger system that can be deterministically examined to solve problems and improve quality.

This book represents a distillation of ideas and concepts that have emerged over 75 years of spindle metrology. The author's interest in spindles began somewhat more recently when he spent a

month during grad school working with Harold Arneson, co-founder of Professional Instruments Company. Harold patiently outlined the fundamentals of metrology while demonstrating the miraculous performance of his air bearing spindles. At that time, the measurement tools were not yet good enough to repeatably resolve the performance of high-quality air bearing spindles as the measurement noise floor was greater than their error motion. In the years that have followed, sensors and data acquisition have caught up and now offer nanometer-level performance. The remaining limitations to air bearing spindle performance are external to the bearing itself: structural vibration, air supply pressure fluctuations, and motorization effects. The author is continuing research on these issues to this day.

Much of the author's research is sponsored by industrial partners seeking to improve the quality of precision machines and instruments. Dave Arneson, Mel Liebers, Steve Sanner, Dan Oss, Ryan Fuchs, Jeremy Ferrie, and Mike Olson at Professional Instruments Co. of Minneapolis, Minnesota and Don Martin, Ray Herbst, and Mark Kretschmar at Lion Precision of St. Paul, Minnesota have provided tireless support and expertise to this work. Mel Liebers spent countless hours explaining and discussing any and all ideas related to spindles and spindle metrology. None of this work would have been successful without the advice, enthusiasm, and 24/7 technical support of David Arneson of Professional Instruments Co. Many thanks to Dave, Mel, and Don and all who have been so generous with their time and resources to bring this book into fruition. Kistler, Corning Tropel, Moore Tool, Edge Technologies, Aerotech, NSF, NIST, and many others have also contributed generously with financial support, time, and equipment.

The author has benefited from additional help from a long list of friends including R. Ryan Vallance, James Flinchbaugh, Alex Slocum, and Matthew Van Doren as well as Penn State colleagues H. Joseph Sommer and Martin Trethewey.

Graduate students Robert Grejda and Jeremiah Couey made the measurements shown in the pages that follow. Both Bob and Jeremiah have the gift of patience, creativity, and tenacity to solve measurement challenges as they arise. These two were kept motivated by many other graduate students in our research lab struggling with their own challenges and successes. When chasing after nanometers, it sure is nice to have folks this good following up on every last detail.

Eric Marsh  
mdrl.mne.psu.edu  
Penn State University  
Aug 2007

# Chapter 1

## Introduction

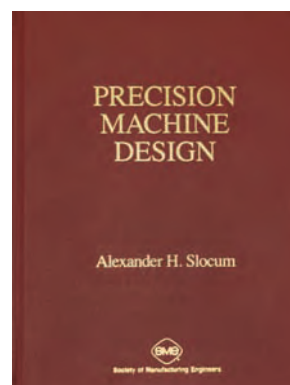
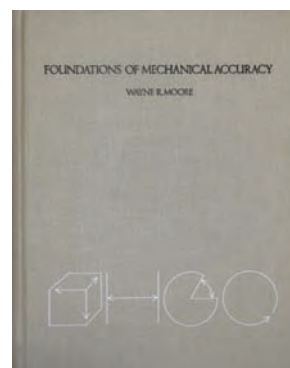
This book provides concepts and measurement techniques for analysis of spindle performance. A practical approach to spindle metrology, as well as real test hardware and data, are used throughout. The reader will gain insight into how to use and measure spindles to improve manufacturing and inspection processes. The book is written for anyone with an interest in spindle performance with emphasis on rotational accuracy. Our goal is to provide a deeper understanding of spindles and their interaction with precision machines, so that the reader can make informed decisions that improve quality.

Although we begin with the basics in our examination of spindle metrology, the reader will benefit from an appreciation of the challenges of working at the nanometer level. Two books that provide excellent introductions to precision engineering are *Foundations of Mechanical Accuracy* and *Precision Machine Design*. Additional resources are listed in the appendix.

### 1.1 What is a spindle?

In its most general form, a spindle is a device that provides for rotation between components. Examples are found in machine tools, metrology instruments, and rotary tables. Relative motion is provided by one or more bearings that provide stiffness, load capacity, and accurate and repeatable rotation. A spindle may be long and slender for high speed or low-profile, such as a rotary table. Or, it may be a workpiece between centers or perhaps a gimbal, a knife-edge pivot, or a pair of trunnions intended for only a few degrees of rotation. Whatever the shape, a spindle has a rotor, a stator, and bearings in between. Figure 1.1 shows a high-speed spindle with a capacitive sensor in place to measure displacement during rotation.

An ideal spindle allows motion in a single degree of freedom: pure rotation. Any movement in the remaining five degrees of freedom is undesired and may be classified as either spindle error (i.e., motion that results from the spindle's design and manufacturing) or as a



Two fine books that introduce the fundamental concepts of precision engineering are *Foundations of Mechanical Accuracy* by Wayne Moore, Moore Tool Co., 1970 and *Precision Machine Design* by Alexander Slocum, Society of Manufacturing Engineers, 1992.

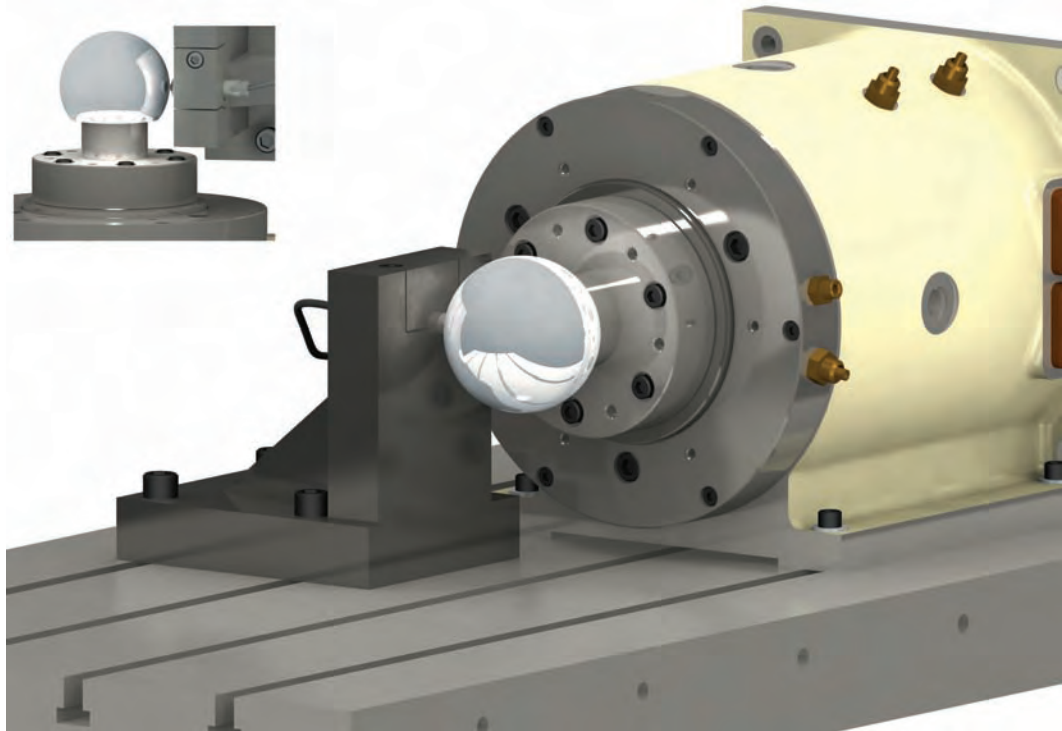


**Figure 1.1** Professional Instruments TWIN-MOUNT air bearing spindle with integral liquid-cooled brushless-DC motorization. A Lion Precision C23-C capacitive sensing probe and CPL290 dual-range probe driver measure with sub-nanometer resolution, 0.3% full scale linearity, and 15 kHz bandwidth against the lapped ball. This particular spindle shows less than 20 nm radial and 5 nm axial error motion at 10,000 RPM.

Some modern capacitive sensor systems now offer the flexibility of dual sensitivity for coarse and fine measurements. Typical sensitivities of the Lion Precision Elite Series are 50, 500, and 2000 mV/micrometer. Measurements like those shown in this book may be taken with 8 mm C23-C probes and Lion CPL modular probe drivers.

response to an external influence, such as thermal gradients, applied forces, external vibration, or some other-named load.

With reliable measurement results in hand, it is possible to search out and identify root causes of these motions. The list of influences that may cause apparent spindle error motion is quite long, and many of these contributions, with some investigation, will prove to be completely unrelated to the spindle. For example, a measurement may be affected by environmental influences, such as floor vibration, acoustic noise, and electrical noise. In other situations, the spindle is simply reacting in a deterministic way to external influences, such as changes in temperature, load, speed, air supply pressure, and direction of rotation. What we desire is a way to specify, measure, and analyze the system so that measured results may be traced to root causes, consequences can be predicted, and improvements made.

Our ability to design, manufacture, and test spindles of ever-increasing quality requires inspection equipment with reasonable resolution, stability, and bandwidth to reliably quantify performance and reveal areas for improvement. Cost is also a consideration because ideally we would like to measure as many as five degrees of freedom simultaneously. Capacitive sensing technology meets each

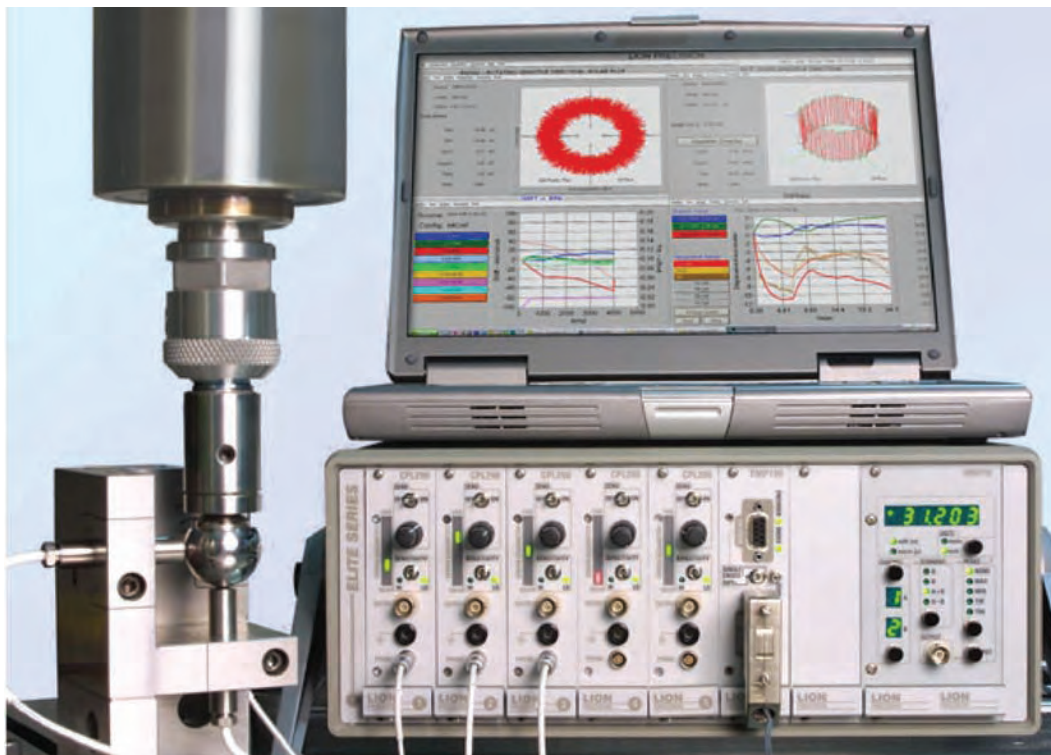


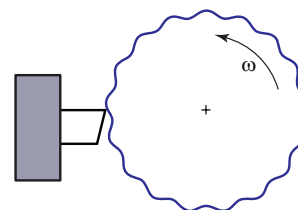
**Figure 1.2** The Spindle Error Analyzer from Lion Precision. This is a turnkey metrology system complete with lapped spherical artifact, five-channel capacitive sensor system, data acquisition card, and Lion SEA software that guides the user through the measurement of spindle motion and thermal response, even when a rotary encoder signal is not available.

of these requirements and can be packaged in robust stainless steel probes. The best commercially-available capacitive sensor systems integrate a shielded and temperature-compensated electrode with signal sensing and conditioning electronics to achieve sub-nanometer resolution over a typical measuring range of 10 to 100 micrometers.

## 1.2 Case study: CNC lathe

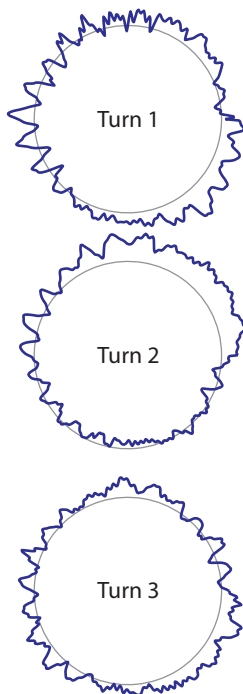
Perhaps the best way to begin a study of precision spindle metrology is by example with familiar hardware. In this case study we examine the radial error motion of a 4 kW CNC lathe spindle. Radial motion is particularly important in outer and inner diameter turning operations because any motion in the normal direction of the cutting tool will correspond to a one-for-one size error in the workpiece.

In later chapters, we will investigate the details of the sensors, fixturing, data acquisition, and processing to capture data of sufficient fidelity to characterize precision spindles. For now we will note that the radial error motion of a CNC lathe spindle is relatively large compared to the out-of-roundness of a high quality lapped spherical artifact; the roundness at the equator of a lapped ball can be as low



End view of a workpiece turned on a spindle with a defect occurring at 17 times the spindle speed.

The grating resolution of a typical encoder is on the order of 1000 counts per revolution. It is possible, although usually not necessary, to interpolate this signal to generate much higher numbers of counts per revolution.



Three consecutive revolutions of lathe spindle data. Although the three revolutions appear to show a certain amount of random behavior, the spindle is actually surprisingly repeatable and will nearly perfectly repeat this path if turned back to the same starting point and remeasured.

as 25 nm or less. This will allow us to neglect the contribution of the target artifact form error and attribute the measured displacement to radial error motion in the spindle and support structure. In this example, the radial error motion is measured with a capacitive sensor system using a probe that is rigidly mounted on the machine. If our aim is to focus on the spindle such that the measurement only reflects its contribution, the fixturing would be bolted directly to the stator. This arrangement minimizes the influence of structural motion and vibration on the measurement. If we are more interested in the motion in the entire structural loop, we might use fixturing to place the probe on the cross slide of the lathe. In practice there is quite a bit of work involved in making fixturing of sufficient rigidity to not influence the measurement, but we ignore these issues for the time being.

The most convenient way to acquire data is using a spindle-mounted encoder to trigger the sampling. Rotary encoders output two digital or analog waves indicating both the direction of rotation and passage of the encoder graduations. Triggering off the encoder bypasses the issues associated with time-based sampling in the presence of spindle speed fluctuations. Rotary encoders also provide an additional once-per-revolution index pulse that allows consecutive measurements to be aligned with each other. Most production machine tools do not allow convenient access to encoder outputs, so the data are sampled in time and synchronized in software.

## Results

Figure 1.2a shows 32 revolutions of unprocessed data taken on the rotating lathe spindle with the capacitive sensor oriented to measure displacement in the radial direction. Closeup views of three revolutions are shown in Figure 1.2b and 1.2c to illustrate some recurring features of spindle measurement data.

First, there is a repeating periodicity in the measured waveform corresponding to a once-per-revolution eccentricity of the target artifact on the spindle. The displacement sensor is measuring against a spherical target surface that is not perfectly centered on the axis of rotation. The sensor sees this eccentricity as a once-per-revolution sine wave. This sine wave is referred to as the fundamental component and is not considered to be an actual error in radial measurements because it can be altered by simply re-centering the target artifact on the axis of rotation. In practice, it is not possible to perfectly center the target, so the fundamental component of radial data is removed in software during post processing.

A similar, but slightly different, situation arises when measuring axial and face displacements. In axial measurements (i.e., measurements collinear with the axis of rotation) the target surface cannot be centered or tilted to remove the fundamental component. The funda-

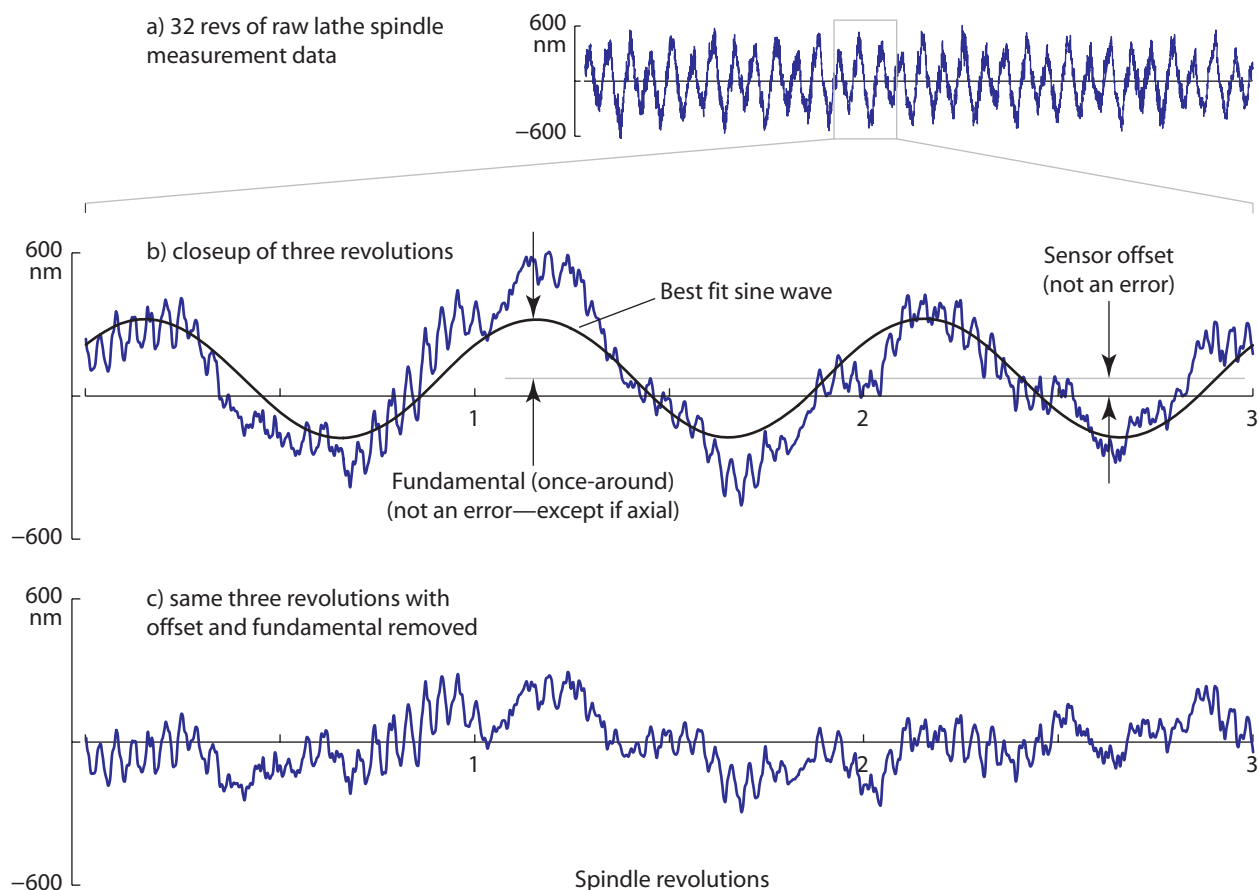


**Figure 1.3** a) 32 revolutions of raw CNC lathe spindle data containing several interesting features for consideration. b) A closeup of three revs containing an arbitrary DC offset reflecting the standoff distance of the displacement sensor to the target surface. This offset is always removed from the data. A once-per-revolution sine wave is also evident in both a) and b). This sine wave may be reduced in radial and face measurements by re-centering or tilting the artifact. In the case of radial measurements, this component is not an error and may be removed completely in post-processing, as in c). The sine wave is handled differently in face measurements as discussed later.

mental component of an axial measurement is therefore a meaningful quantity. In face measurements (i.e., parallel to, but offset from the axis of rotation) the target surface, which is perpendicular to the axis of rotation, may be tilted to arbitrarily change the fundamental component. However, the apparent fundamental component will be different at a new radial location of the measurement. The best that can be done is to adjust the tilt of the artifact until the fundamental component is the same at all radial locations, including the on-axis axial measurement. The resulting fundamental motion looks like a piston-type oscillation of the spindle along the axis of rotation. In practice, we do not usually take the time to micro-adjust the artifact tilt to the nanometer level, but rather remove the fundamental component from the face measurements in software and report its amplitude separately.

The fundamental component, in the specific case of axial mea-

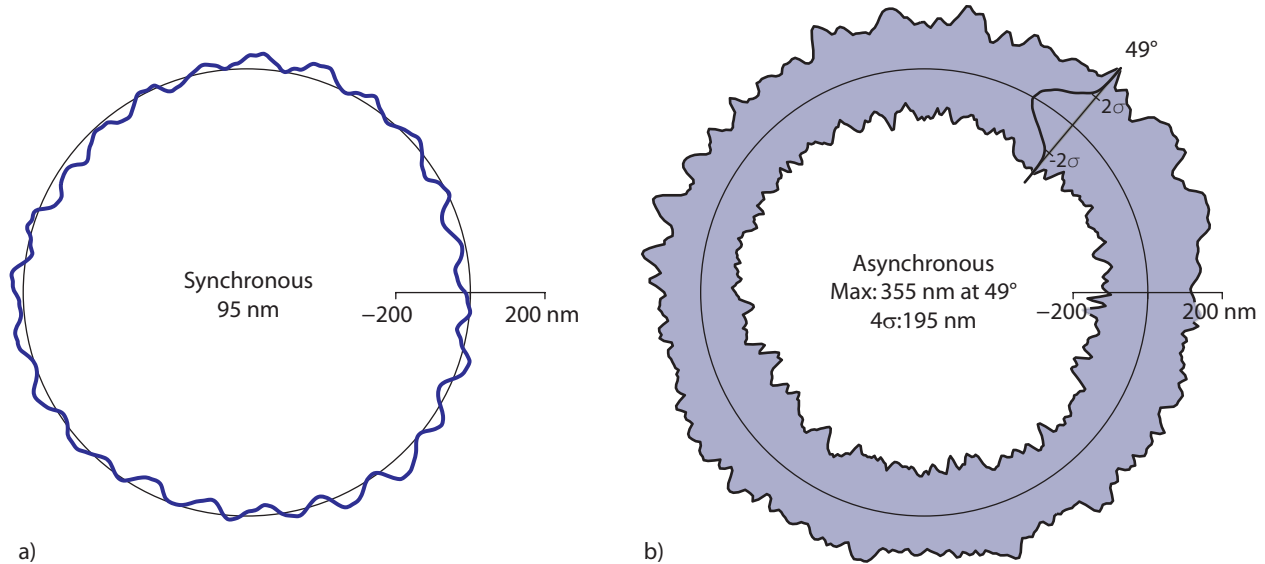


**Figure 1.4** The a) synchronous and b) asynchronous radial error motion of a CNC lathe spindle over 128 revolutions. As will be shown, the asynchronous error is not random, but is in fact a repeatable error occurring at non-integer multiples of the spindle rotation. The majority of error motion in ball bearing spindles is usually asynchronous.

Spindle balance problems may manifest themselves as fundamental axial structural motion. An easy way to detect balance problems is to run tests at multiple speeds and look for varying amplitudes of fundamental axial error.

See Tlusty's "System and methods of testing machine tools" in *Microtechnic*, 13:162-178, 1959 for examples of the first polar plotted spindle measurement data.

measurements, reflects a legitimate error motion of the spindle. In contrast, the fundamental component seen in face measurements can be reduced at all radial locations simultaneously to the level of the fundamental seen in axial measurements by appropriately tilting the artifact. As with the radial measurements, it is important to distinguish the effects of arbitrary centering and tilting of the artifact from the error motions of the spindle.

The second feature of the data plotted in Figure 1.2b is the DC offset of the data set. This offset is an artifact of the arbitrary probe standoff distance and its driver electronics and is not meaningful in a spindle measurement. Figure 1.2c shows the measured waveform after the once-per-revolution and DC offset are removed.

Error motion data are conveniently graphed on a polar plot, as originally suggested by spindle metrology pioneer George Tlusty in 1959. By plotting multiple revolutions of measurement data, an average (synchronous) pattern emerges, as shown in Figure 1.2a. This synchronous component may then be subtracted from each revolution of the original data; the remaining asynchronous component is shown in Figure 1.2b.

Polar plots emphasize several important characteristics of the spindle, including low-order lobing and higher-order waviness in the synchronous error motion, the width of the asynchronous cloud band, and the various error motion values shown tabulated inside the plot. In fact, appropriately-scaled polar plots are particularly helpful to the metrologist seeking root causes for observed behavior. Identification of periodicity, or lack thereof, allows rapid identification of the

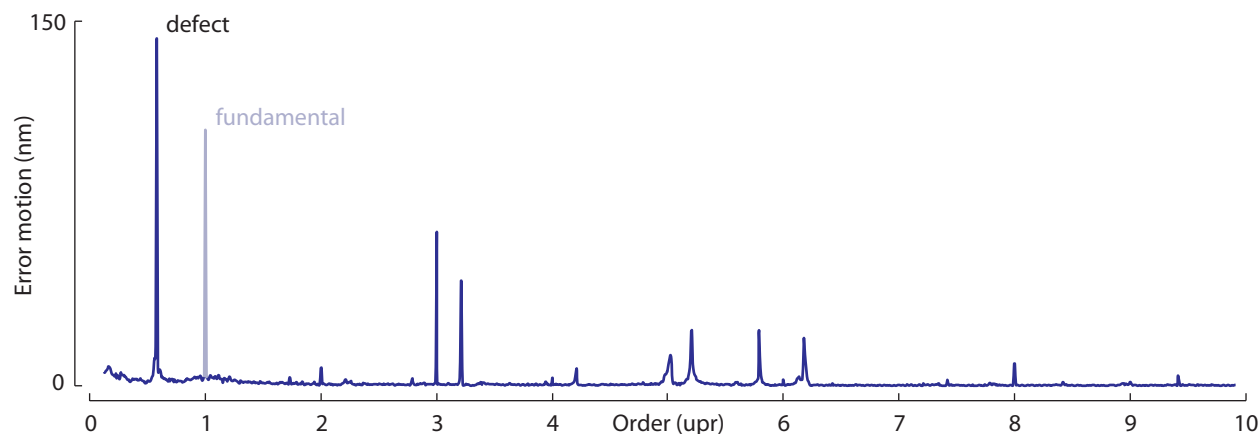


**Figure 1.5** FFT plot revealing specific ball bearing defect frequencies including a defect at 58% of the shaft rotation frequency. The frequency resolution is quite good in this particular plot because the displacement is measured for 128 revolutions. Note that the fundamental component at 1 upr is removed in this radial measurement.

source of problems by process of elimination.

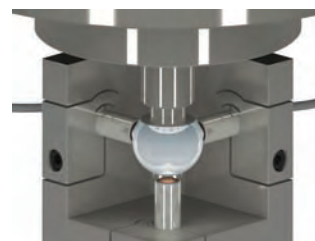
In this lathe spindle example, radial motion is shown for 128 revolutions with synchronous error of 95 nm. The asynchronous error motion value is 355 nm, which defines the maximum range in the measurement at any one angular location over the 128 revolutions. In many applications, the maximum excursion of the asynchronous error motion is critically important, but it is worth noting that the asynchronous error motion often falls in a roughly normal distribution. In this example, most (95%) of the asynchronous values fall within the 4 standard deviation ( $\pm 2\sigma$ ) range of just 195 nm.

The synchronous error motion limits the form error of workpieces turned on this lathe. Figure 1.2a shows a 24-lobe feature in the synchronous error. It is unlikely that this particular component of the measurement is due to a ball bearing defect because such defects generally give rise to frequency components at non-integer multiples of spindle rotation. The 24-lobe error is more likely due to the motor-pole cogging or other effects of the spindle drive. This sample lathe measurement shows significant asynchronous error as is typical of ball bearing spindles; the synchronous error motion of ball bearing spindles is usually smaller than the asynchronous component.

To gain further insight into the asynchronous component of the measurement, Figure 1.2 shows the FFT of the radial error motion computed from the 128-revolution test. Although polar plots are very effective at conveying certain aspects of the error motion, the FFT is invaluable for identifying the defect frequencies that occur as predictable functions of the bearing geometry including ball diameter, the number of balls, inner and outer race diameters, and contact angle. The FFT plot of error motion is a good place to start, when troubleshooting, because the individual fault frequencies can be matched to specific bearing geometry defects. In this case, the largest single

Bimodal distributions are also possible in rolling element spindles as a result of errors occurring at the cage rotation frequency.

It is possible to turn shiny parts on a spindle with significant synchronous error provided that the asynchronous error is low. Only by careful measurement will the workpiece form error be revealed. Synchronous error defines the shape of the workpiece while asynchronous error motion limits the achievable surface finish.



error component occurs at a frequency 58% of the spindle rotation speed.

It is also possible to measure the thermal response of the CNC lathe by setting up probes to record the tool-to-workpiece separation over a longer period of time, typically measured over hours rather than seconds. As the lathe reaches its equilibrium operating temperature, there will be a corresponding expansion of the machine structure. Thermal growth is caused by more than just the heat generated by friction and motor losses in the spindle. The structural design and heat sources of the entire machine and its environment lead to temperature gradients that appear as growth or drift in the measurements, depending on the placement of the displacement indicators. As every machinist knows, part size will vary during warm-up, because the machine's encoders are not sensitive to localized temperature gradients in the machine and cannot compensate for this transient source of error.

### 1.3 Brief history of spindle testing

#### Early testing techniques

The modern era of systematic testing of machine tools began with Schlesinger's tests for quantifying the performance of machine tools. Schlesinger is credited with publishing the first comprehensive battery of tests to assess the performance of a wide variety of production machines. A translation of Schlesinger's 1927 work first appeared in English as *Inspection Tests on Machine Tools* in 1932. The revised edition, *Testing Machine Tools* outlines a well-defined series of methods for acceptance testing of production machine tools. These tests used mechanical displacement indicators, axial "slip," and other quantitative methods. The importance of using high quality gaging surfaces on machine tools for measurement. These tests are dependent on the

Georg Schlesinger (1874-1949) received his doctorate in 1904 at the Technischen Hochschule (later renamed Technische Universität) Berlin, and his research on restructuring and improving many facets of production processes led to his appointment to the post of Director of the Royal Gun Factory in Spandau until 1934. He fled Germany prior to WWII and eventually settled in Great Britain after the English publication of his seminal work *Testing Machine Tools*.



## Chapter 2

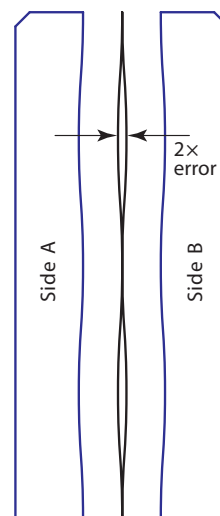
# Spindle Metrology Concepts

This chapter introduces the concepts necessary to describe the error motion of a precision spindle. One of the foundational ideas is the distinction between runout of the surface of a spinning artifact and spindle error motion. This idea was briefly mentioned in Chapter One when Schlesinger's early work was discussed. The issue is that a displacement indicator targeting a rotating surface measures the combined contribution of the spindle error and the imperfections of the target surface. In subsequent chapters, error separation techniques will be introduced to separate the two contributions. For now it is important to bear in mind that the measurements we make will require a certain amount of additional testing as well as postprocessing, if the form error of the artifact is significant compared to the spindle error.

Figure 2 demonstrates this concept in the case of a measurement made against a surface with errors of roughly the same magnitude as the spindle. In this example, error separation reveals radial spindle error motion that is completely different from the form error of the artifact.

As we introduce the fundamentals of spindle metrology, we will assume that the contribution of the artifact is small compared to the spindle error motion. This means that in the examples that follow essentially all the measured displacement is assumed to be due to the spindle and other influences because the artifact is taken to be comparatively better. This assumption is often valid for measurements made on ball bearing spindles. Such a spindle may have micrometer-level error motions. If the artifact is a typical lapped sphere with a form error of perhaps 25 nanometers, it will usually be sufficient to neglect its contribution to the measurement.

In situations where it is not possible to neglect the contribution of the artifact, an error separation procedure must be applied to the measured data. Once the contribution of the artifact has been



Perhaps the simplest reversal to visualize is used for straight-edges. Rather than rely on a comparison to some master artifact, the error is revealed by the difference in edge contours before and after flipping the scale. The width of the difference between the two is twice the straightness error. Clever use of reversal allows a measurement to be self-checking, a principle that is beautifully illustrated in Wayne Moore's *Foundations of Mechanical Accuracy*.

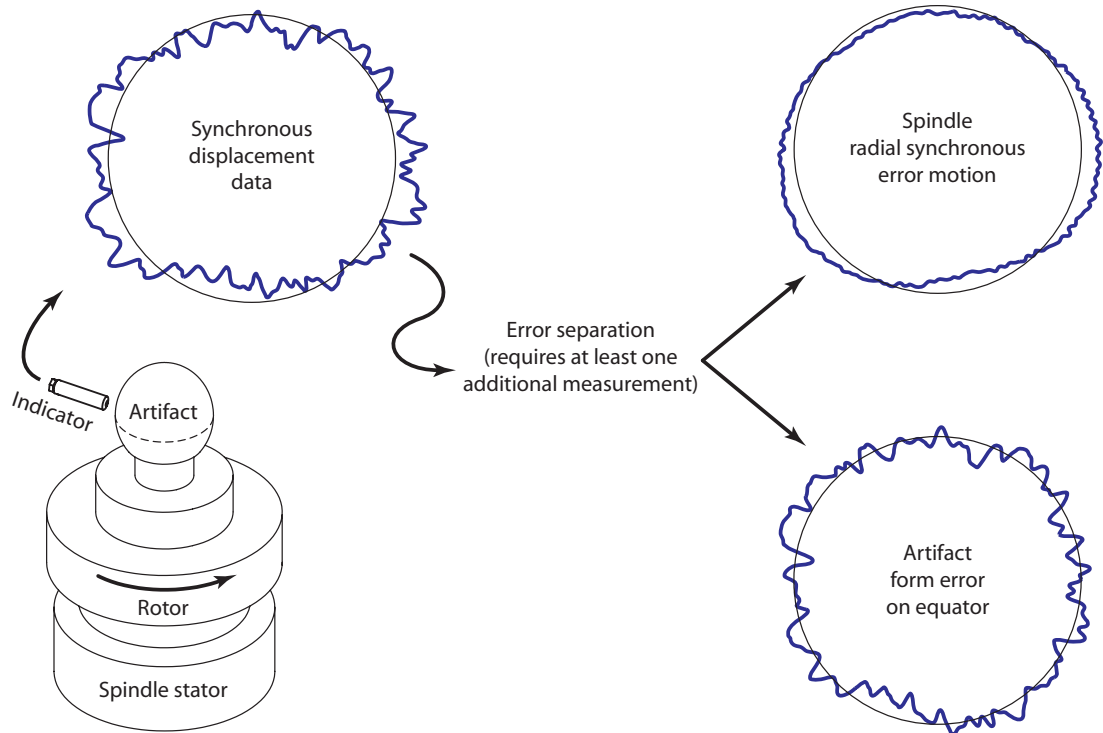


**Figure 2.1** A preliminary look at the separation of a displacement measurement into spindle and artifact errors. Note that separation requires one or more additional measurements.

extracted, the concepts introduced in this chapter may be used.

## 2.1 Spindle fundamentals

The terms to unambiguously describe the performance characteristics of a precision spindle will be introduced using data from a PI ISO 5.5 air bearing spindle as shown in Figure 2.1. This particular spindle is driven by a frameless, brushless DC motor and uses externally-pressurized air in a thin gap between the rotor and stator to provide nearly frictionless rotation. There is no mechanical contact between the stator and rotor, and the air film produces an averaging effect that attenuates the geometric imperfections in the spindle components. Heat generated in the spindle is efficiently removed with water cooling.

One of the most interesting aspects of air bearing design is the compensation of the air flow such that a restoring force will always tend to push the rotor back to its equilibrium position. In practice, air bearing spindles have compensation based on orifices, porous media, steps, or grooves. Air bearing spindle design requires a thoughtful compromise of many competing requirements.

A perfect spindle would provide pure frictionless rotation with zero motion and infinite stiffness in the remaining off-axis directions (two more rotations and three translations). By this definition, we will have to get used to the idea of dealing with imperfect spindles. Fortunately, the ASME B89.3.4 standard outlines an entire vocabulary to describe spindle imperfections clearly and precisely.

Many of the key concepts of spindle metrology may be understood by considering spindle error motion in each of three different

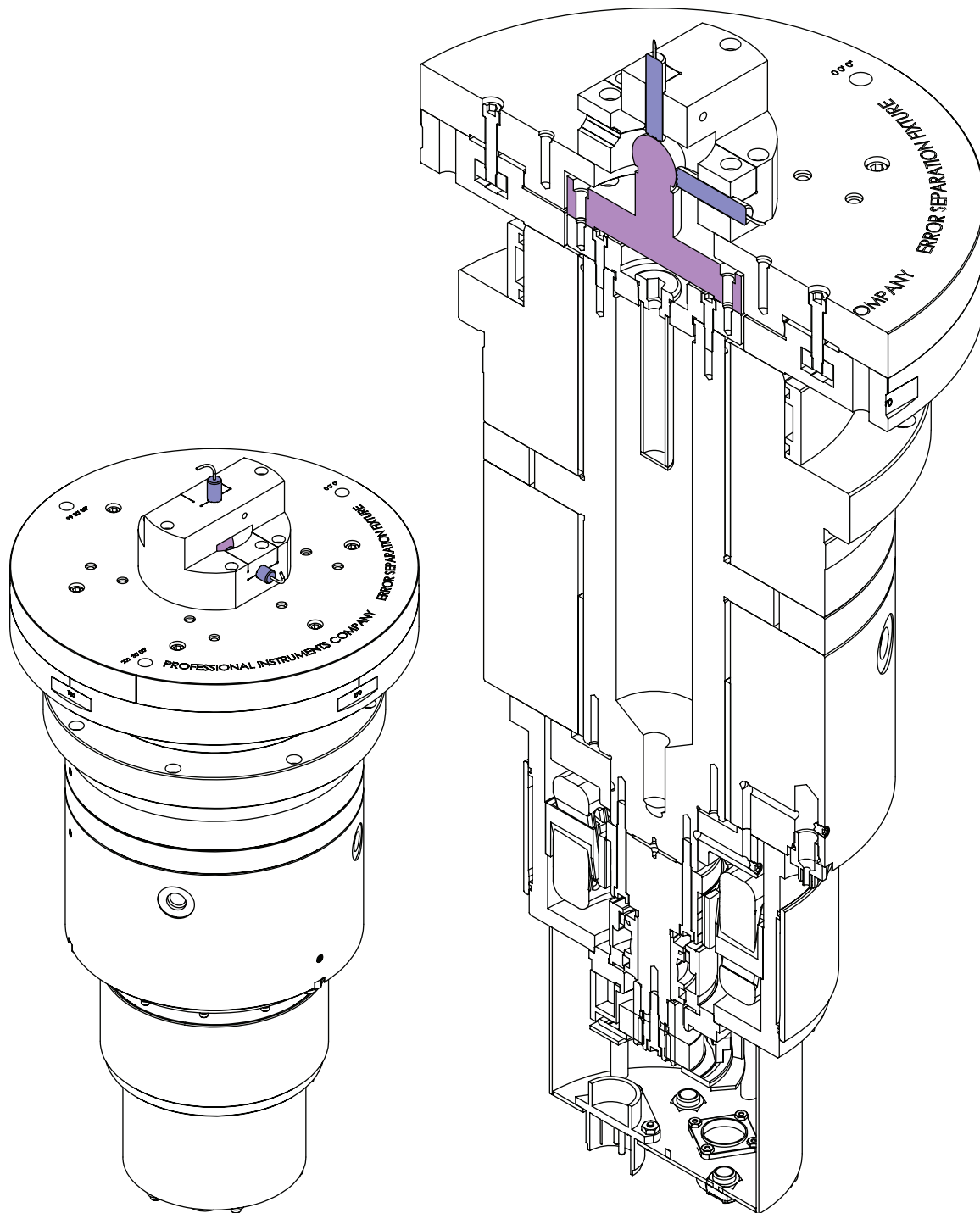


**Figure 2.2** A PI ISO 5.5 high-speed air bearing spindle with integral frameless, brushless DC motor and optical encoder. Every detail of this spindle package has been carefully optimized to reduce its error motion to less than 25 nm at speeds up to 10 kRPM. The artifact and probe mounts are designed to be as rigid and close to the spindle as possible so that the spindle error may be measured without including the influence of a large structure. Fittings are provided for water cooling to compensate for any heat generated in the air film and motor windings. Brushless motors are best for precision applications because their high efficiency reduces the amount of heat generated.

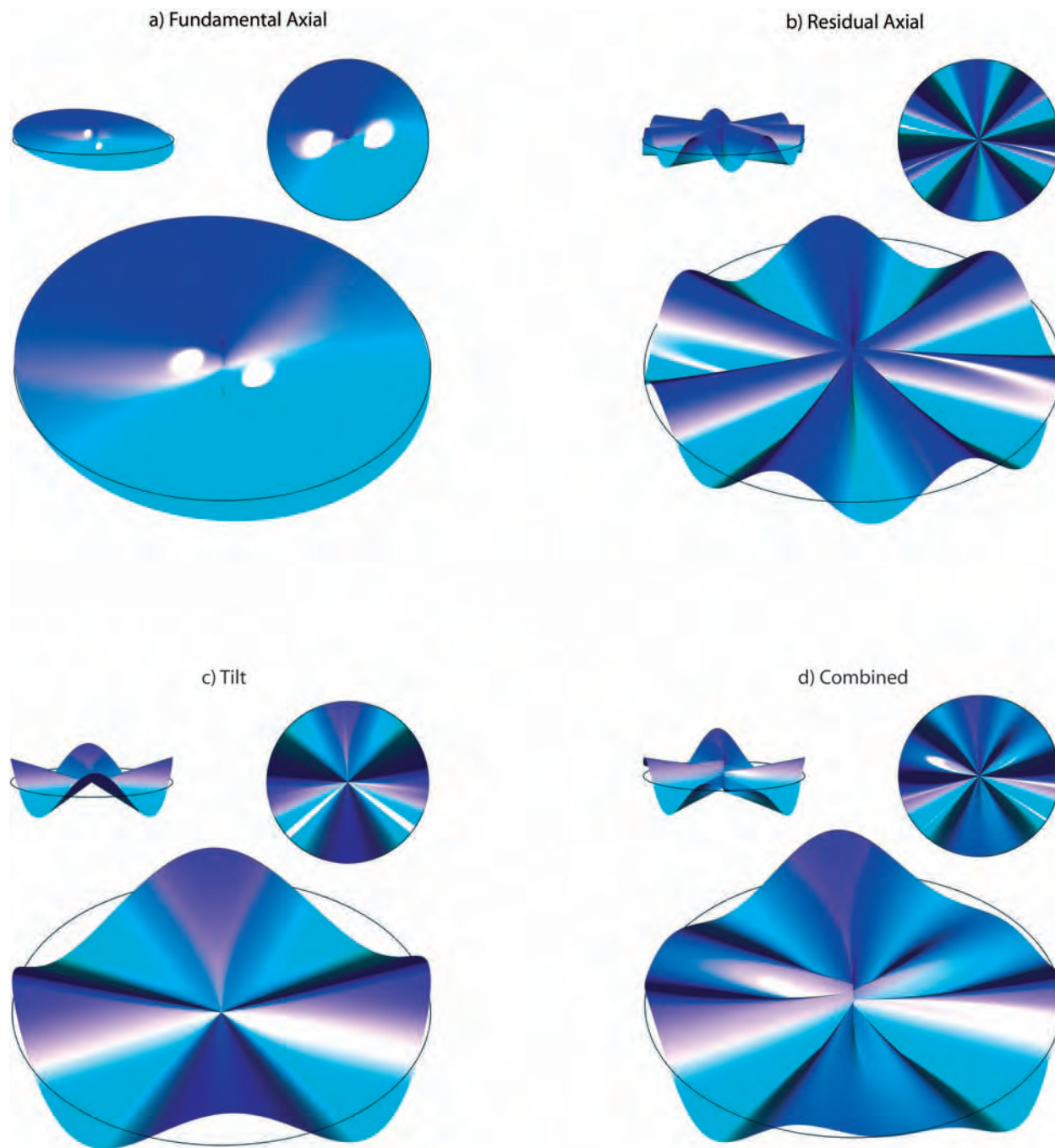


**Figure 2.6** Exaggerated profiles of workpieces face-turned on spindles with a) fundamental axial, b) residual axial, c) tilt, and d) combined axial and tilt error motion. Note that the workpiece turned on tilt error motion spindle c) has zero form error in the middle, while the residual axial error motion spindle b) does not converge to zero error on the centerline. These profiles are the result of synchronous errors.



**Figure 2.7** Exaggerated profiles of workpieces turned on the outer diameter on spindles with a) tilt extending from a location with zero radial, b) radial in the absence of tilt, and c) combined radial and tilt error motion. An important distinction between a) and c) is that spindle a) has an axial location at which the radial error motion is precisely zero. In practice, this is not likely. In general, the radial error reaches a non-zero minimum at some axial location, as in c). Asynchronous error affects the surface finish, in addition to the effects of the synchronous error motion shown here.

poorly designed drive systems and excessive thermal and mechanical loads from external (and usually preventable) sources. It is critically important that the metrologist appreciate the distinction between intrinsic and external sources of problems and always approach spindle measurement results with an eye for properly identifying the root causes. For our purposes, it is useful to consider the entire motorized spindle package as the spindle.

All spindles have compliance and coefficients of thermal expansion. Therefore, the spindle will respond in a predictable way to mechanical and thermal loads. Some of these loads are inherent to the operation of the spindle. For example, the friction in a running spindle will lead to heat, which in turn leads to growth dependent upon the properties and geometry of the spindle. The response of a particular spindle to this inevitable effect is an important characteristic to consider when evaluating its design.

The B89.3.4 Standard provides the framework for evaluating spindle error motion, compliance, and thermal response. In general, these three quantities are measured and reported separately. However, a spindle marketed with an integral motorization should appear

Richard F. Moore, founder of the Moore Special Tool Company, describes how an electric resistive spindle heater may be used to great benefit in jig grinder spindles in his 1955 book *Holes, Contours, and Surfaces*. In 1974, American Machinist awarded Richard Moore the AM Award recognizing him as the man who “gave the world’s industry an additional decimal place of accuracy!”



## Chapter 3

# Test Instrumentation

This chapter introduces the equipment needed to carry out measurements that accurately capture the behavior of a spindle:

- spindle (possibly with rotary encoder for synchronization)
- suitable artifact
- displacement sensor(s) and fixturing
- data acquisition, processing, and storage hardware (Chapter Four)

Figure 3 shows a setup for measuring fixed sensitive direction radial motion. The spindle is rigidly mounted on a T-slot table as is a displacement indicator with a sturdy bracket. The capacitive sensor driver electronics output a  $\pm 10$  V analog signal proportional to the distance between sensor and target with 15 kHz bandwidth. This signal could be monitored with an oscilloscope, but in practice it is usually digitized, analyzed, and stored using a computer with data acquisition hardware and software.

The artifact in this figure is a one-piece lapped stainless steel sphere and flange bolted to the spindle rotor. A high-quality artifact should have a form error less than 25 nm. In many cases, depending on the spindle, this out-of-roundness error will be so small compared to the spindle and structural errors that its contribution may be safely neglected. This is particularly true of ball bearing spindles, which typically have at least 100 nm error motion. Most production equipment and machine tools use ball bearing spindles so the artifact error may be neglected. However, a few air bearing and hydrostatic spindles are so good that artifact form error cannot be ignored. We will skip over the treatment of artifact imperfections until Chapter Four and focus here on the mechanical hardware needed to make measurements.

The fixturing used with metrology artifacts is critically important. The artifact should be permanently attached to a suitable shank, and the shank should be used with a high-quality collet, taper, or flange-mounted tool holder. The best solution is to use a one-piece artifact and shank in the best workholder available. Any slight play in the artifact fixturing will appear as a very large error in a spindle measurement. As obvious as it may seem, this is a very common problem.

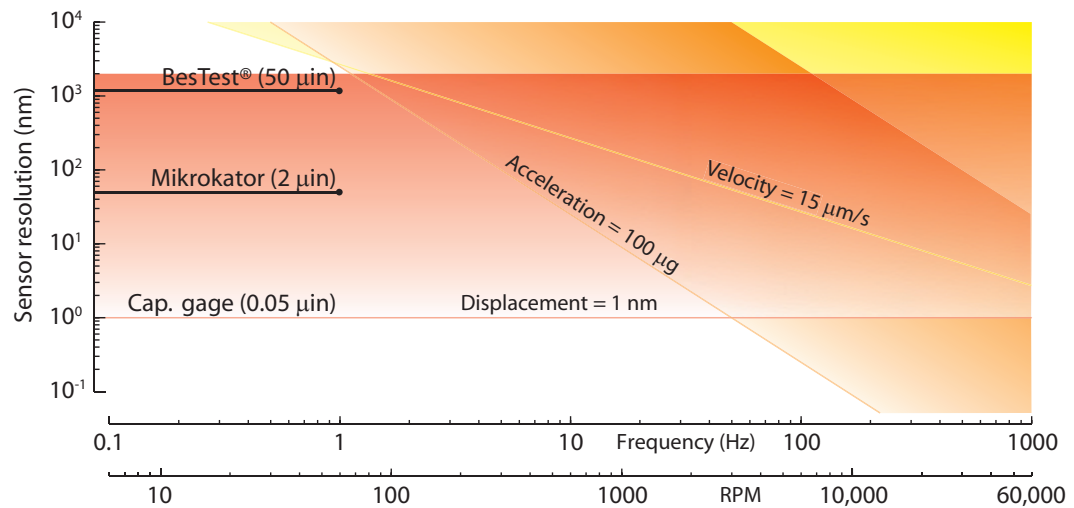


**Figure 3.3** Representative values of acceleration, velocity, and displacement sensor resolutions. Capacitive-type displacement sensors can provide appropriate range and resolution down to 0 Hz. Velocity and acceleration-based sensors surpass the resolution of displacement sensors at higher frequencies, but their low frequency performance is inadequate.

### Rotary encoders

In general, a spindle's speed fluctuates by some amount when running. As will be seen in the next chapter, provisions need to be taken to synchronize the streaming data to the rotation of the spindle. Many modern spindles found in production equipment have rotary encoders, but access to the encoder output may be difficult. In this case, we rely on the slight eccentricity in the mounting of the measurement artifact to provide a once-per-revolution component that identifies the consecutive rotations of the spindle. This is not necessarily an ideal solution because the desired timing signal must be identified from a much more complex signal. However, this is often the only option for testing spindles on production equipment.

We have used 1024 and 4096 count encoders with great success. Lower-count encoders may not provide as much frequency range, but may be necessary for extremely high speed spindles depending on the data acquisition system's maximum sample rate.

An alternate solution that may be suitable in laboratory-type settings is to use a spindle-mounted precision rotary encoder to synchronize the data capture. In this case, the square wave output of the encoder is used to trigger the data acquisition so the data are equally spaced in spindle rotation angle, independent of running speed. The FFT of this data will generate sharp peaks at defect frequencies occurring at multiples of running speed, even if the spindle speed varies during the measurement.

### Motorization

Spindle motorization is an interesting issue because by strict definition, a spindle's response to motor cogging and motor pole print-through is not spindle error motion. This motion is simply a conse-

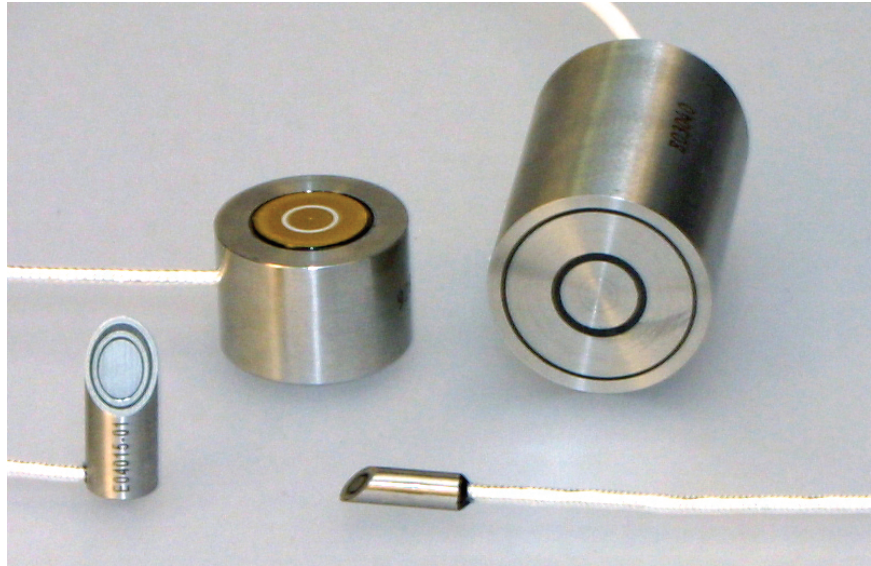


**Figure 3.6** Custom-made capacitive probes from Lion Precision for special applications. These probes are shielded, temperature compensated, and factory calibrated for linear outputs over their measurement range. A comprehensive line of standardized probes is also available from Lion.

Mikrokator (50 nm per division) or the Mahr Supramess (500 nm per division).

The capacitive probe body contains the sensing electrode and a guard ring to shield the electrode from stray capacitance, as shown in Figure 3.8. The sensor is positioned with its sensing electrode parallel to the target electrode (artifact) with the appropriate nominal standoff distance. The measurement range in which a probe is useful is a function of the area of the sensor. The greater the area, the larger the range. Because the driver electronics are designed for a certain amount of capacitance, a smaller sensor must be closer to the target. The electronics are adjustable during calibration, but there is a limit to the range of adjustment.

The conductive sensing and target electrodes operate under a potential difference when separated by a dielectric material (e.g., air). The theoretical (ideal) capacitance  $C$  between two flat and parallel electrodes separated by a small gap is proportional to the permittivity of free space  $\epsilon_0 = 8.854 \times 10^{-12}$  F/m, the relative permittivity of the dielectric material separating the sensor and target  $\epsilon_r$ , and the area of the sensing electrode  $A$ ; the capacitance is inversely proportional to the gap  $g$  that separates the sensor and target electrode:

$$C = \frac{\epsilon_0 \epsilon_r A}{g}$$

The relative permittivity  $\epsilon_r$  is the ratio of the actual dielectric's permittivity to the permittivity of free space. In a vacuum  $\epsilon_r = 1$  and in air  $\epsilon_r = 1.0006$ .

Many of the foundational concepts of instrumentation are described in Kurt Lion's *Instrumentation in Scientific Research: Electrical Input Transducers*, 1959 and *Elements of Electrical and Electronic Instrumentation, An Introductory Textbook*, 1975.



**Figure 3.7** Lion Precision 3-channel CPL290 capacitive probe driver with MM190 LED display. The output from each channel is a  $\pm 10$  V analog signal that can be electronically zeroed at an arbitrary gap distance. This particular modular system is also configured for multi-channel temperature measurement and encoder input using the TMP190 module.

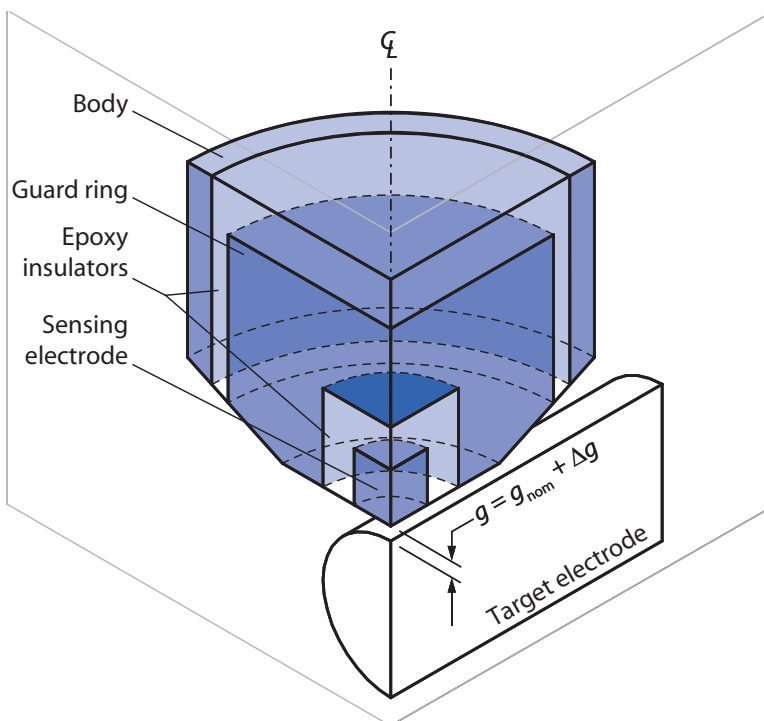


**Figure 3.8** One-quarter of a representative capacitive probe body showing the sensing electrode, a cylindrical target electrode, the guard ring, and conductive body.

### 3.4 Environmental effects

We close this chapter with a brief discussion of the importance of making spindle measurements in a reasonable test environment. The collection of equipment needed to carry out a spindle measurement leads to a considerable exposure to external influences from a variety of noise and energy sources. Unfortunately, any motion in the system, regardless of the source, has the possibility of being incorrectly interpreted as spindle motion. It is not uncommon to discover important facts about a machine tool or metrology instrument when taking a careful look at spindle performance. However, it is not appropriate to categorically assign every component of a measured signal as spindle error.

Perhaps the most frequent culprit in misdiagnosing a spindle problem is unacceptably high compliance in the fixturing used to hold the displacement indicators. The first-time spindle metrologist will be tempted by the ease and convenience of magnetic base indicator stands to place capacitive sensors in position to target the artifact. These magnetic base stands are invariably inadequate for the job of making dynamic measurements on a spindle. Very low-frequency resonances are the norm, and the measurement results will inevitably be quite misleading. Other common issues include:

- inadequate artifact mounting hardware
- temperature fluctuations from insufficient spindle cooling
- temperature fluctuations from poor machine design
- dirt, debris, or fingerprints on the artifact
- improper (or absent) analog filtering
- AC coupling
- interference from nearby capacitive sensors driven by other oscillators
- improper digital filtering
- faulty grounding between the probe body and artifact
- noise from AC servo motors
- ambient vibration
- motion control oscillation between encoder counts
- spindle unbalance
- single-screw hold downs that allow wobbling

The metrologist must investigate the various components of a measurement to sort out how they might trace back to root causes. This exercise is an effective way of learning a great deal about a machine and how it might be improved. In many cases, a spindle test will reveal several low-cost changes to a machine or instrument that may significantly improve performance.



## Chapter 4

# Data Analysis

This chapter introduces techniques and tools used to gather, store, and display spindle measurement data. Chapter Three described the hardware for making spindle measurements up to the calibrated output voltage from the displacement sensor; in this chapter that analog signal is digitized, filtered, and processed.

### 4.1 Data acquisition

We have already looked at using a rotary encoder to synchronize and trigger the data acquisition. There are a number of additional issues associated with processing analog displacement data. Prior to digitization (i.e., analog-to-digital conversion), it is critically important that the signal always be analog anti-alias filtered to remove frequency content above the Nyquist frequency (one-half the sampling frequency). This is the only way to ensure that the frequency components are reliably attributed to the correct frequencies.

Ideally, the data acquisition system will sample all channels of the displacement sensors at the same time. This is an optional feature on commercially-available data acquisition cards, but is common on the higher quality cards that would be used for spindle testing. Simultaneous-sample-and-hold acquisition ensures that multi-channel data sets are properly synchronized. Less sophisticated DAQ cards use a single analog-to-digital conversion chip and sample multiple channels sequentially.

Once anti-alias filtered and digitized, the data may be manipulated with additional digital filtering and other processing algorithms in software. Because this filtering is done after the test data set is completely digitized, it is possible to implement zero-phase-shift filters that avoid artificial distortion to the data. All of these steps are readily carried out with commercially available hardware and software tools.

$$\text{Low-pass filter } X(k) = \begin{cases} \text{unchanged} & : 1 \leq k \leq m \\ 0 & : m < k < N - m \\ \text{unchanged} & : N - m \leq k \leq N - 1 \end{cases} \quad (4.8)$$

### 4.3 Error separation

In the sections that follow, we investigate methods of analyzing synchronous spindle measurements made against an artifact in which the out-of-roundness of the artifact cannot be ignored. Three types of methods will be introduced.



An artifact and three probes arranged to do half of a reversal. Theoretically, the axial probe does not require error separation, as all of the measurement may be attributed to the spindle. But the radial measurements must be repeated with the probe nest and artifact rotated  $180^\circ$  to collect the additional data needed to carry out the reversal calculation. It is often worth recording the axial measurement during each test to verify the repeatability. The average of the axial results can be used to obtain a more accurate result.

**Reversals** require two measurements to compute a single component of spindle error (i.e., radial or face). Both the artifact and displacement indicator must be moved between measurements. Reversal is theoretically superior to other methods, but requires high-quality hardware to achieve nanometer-level results. A good choice for calibrating artifacts at low speed.

**Multistep methods** require many measurements for each spindle error component. Here we do not move the indicator, but instead rotate the artifact in equally-spaced increments. Best left for situations when moving the displacement indicator is difficult.

**Multiprobe methods** use three or four probes to simultaneously measure two orthogonal error components. In this case, neither the probes nor the artifact are moved, but all must be properly arranged to measure the same track on the artifact. A good choice for high-speed applications.

As long as the artifact and spindle error profile measurements are repeatable, each of these methods will give similar results, with a well-documented exception that is explained below. Asynchronous content is neglected in all three approaches.

Measuring either the error motion of a precision spindle or the form error of a rotationally symmetric workpiece is essentially the same task because in both cases the displacement sensor measures a combination of the spindle error motion and workpiece form error. Today's externally pressurized aerostatic and hydrostatic spindles show the same nanometer-level error motion as many of the precision workpieces that need to be measured; neither contributor can be ignored.

Ideally, a complete and accurate separation correctly assigns all synchronous components in the recorded data to the spindle or artifact in the correct proportion. Reversal methods, proposed by Donaldson and Estler, result in complete separation of the workpiece

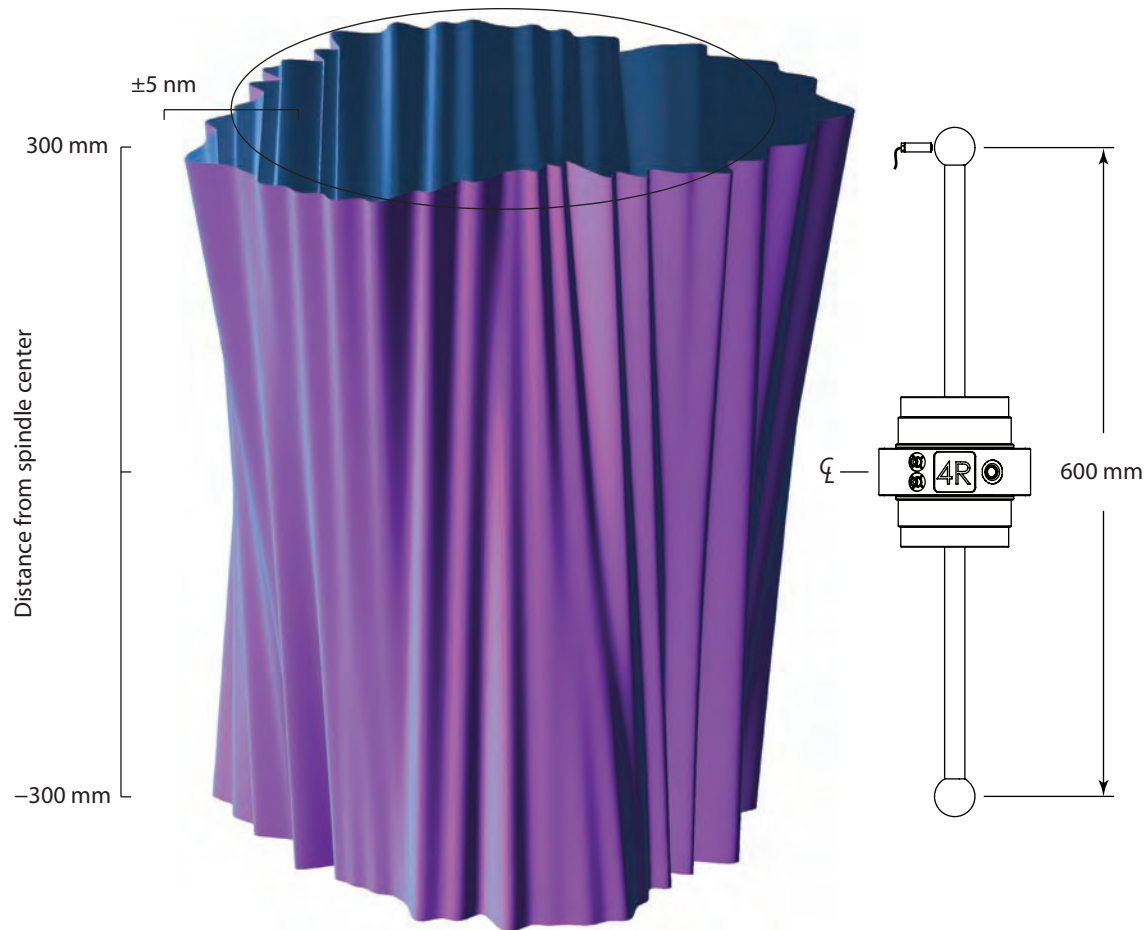


**Figure 4.8** A 3D representation of measured radial plus tilt error motion (fixed sensitive direction) at locations ranging up to 300 mm on either side of the PI 4R spindle. The tilt error motion causes the radial error motion to slowly grow at locations farther away from the spindle (from 5 nm at the rotor to 13 nm at 300 mm out).

form errors from the spindle error motion within the limitations of only time, money, and skill.

Figure 4.3 and 4.3 show fixed sensitive direction results taken on a PI 4R spindle using 0.4 mV/nm Lion Precision capacitive sensors. These sensors have more than enough resolution to capture the nanometer-level characteristics of the extremely accurate rotation of the PI spindle. The figures were made using Grejda reversal, a modification of Donaldson reversal described later in this chapter.

Multiprobe and multistep methods are considered error separation techniques rather than true reversals. These two families of techniques cannot and do not completely separate the errors from spindle and workpiece, but are still used in many situations. Both classes of multi-position methods (i.e., multistep and multiprobe) model errors with a Fourier series, use redundant measurements for the benefit of error reduction through averaging, and incorporate circle closure to

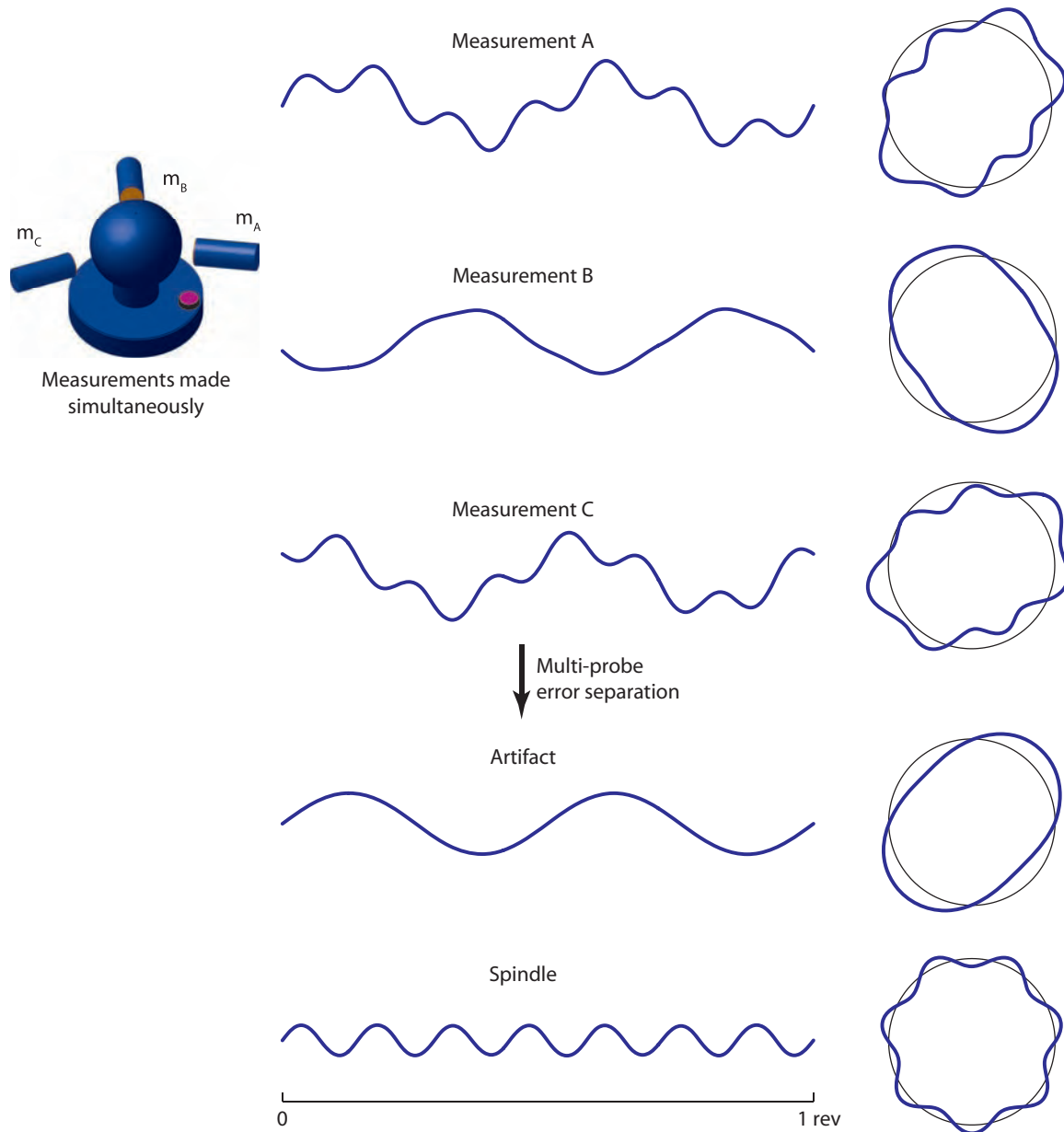


**Figure 4.16** Simultaneously captured measurements  $m_A$  through  $m_C$  in a multiprobe error separation (simulated). The results show perfect separation of the errors of an artifact with 2-lobe form error and a spindle with 7-lobe radial error. In multiprobe error separation, some frequencies will not be correctly separated. The affected frequencies are predictable and depend on the angles between probes ( $\phi$  and  $\psi$ ).

## Chapter 5

# Production Equipment Case Studies

In this chapter we consider four case studies demonstrating measurements of spindle and structural error motion. The first three are taken on production machine tool spindles with displacement indicators arranged to span the entire structural loop from workpiece to tool. The fourth case study outlines the issues required to isolate the spindle from the larger structure using specially-designed probe holders and fixturing. The four case studies are:

**Surface grinder** A manually operated  $150 \times 450$  mm surface grinder with a single-speed, ball bearing spindle. The relevant measurement is fixed sensitive direction radial error motion at the axial location of the grinding wheel. The appropriate measurement requires a single, vertical displacement sensor at the orientation angle of the wheel/workpiece contact.

**CNC turning center** This slant-bed lathe has a  $250 \times 500$  mm workpiece capacity and a 4000 RPM, 15 kW spindle. The lathe does not have a turret-mounted live spindle, so the cutting tools contact the work in a fixed sensitive direction. Three displacement indicators are needed to characterize its motion; two are oriented radially and one sensor is oriented in the axial direction. From this information we can calculate the radial and face error motion at any tool location.

**CNC machining center** This vertical-spindle milling machine has a  $750 \times 400 \times 500$  mm work envelope and a 7500 RPM, 15 kW spindle. Depending on the application, a fixed or rotating sensitive direction approach may be the most appropriate. In either case, five sensors are needed to fully characterize the spindle to handle all milling, boring, and drilling operations.

**CNC diamond turning machine** This horizontal-spindle diamond turning machine features a 6000 RPM spindle with radial

error motion less than 50 nm throughout its entire operating speed range.

This chapter demonstrates the fixturing and setups used to make the measurements. In every case, extra effort put into the setup and fixturing leads to significant time savings once testing gets underway. Other issues to consider include:

- The indicators may not be perpendicular to the artifact.
- The indicators may not be lined up properly on the equator of a spherical artifact.
- Structural vibration may cause motion that looks like spindle error.
- The apparent artifact surface is filtered by the indicator tip or capacitive electrode size (this is often a benefit—short wavelength spindle errors are visible, but short wavelength artifact errors are attenuated).
- Rotating sensitive direction test results differ from fixed sensitive direction results.
- Artifact form errors may add or subtract from the spindle error motion at a given orientation.
- The artifact may be loose or poorly mounted on the spindle (often seen as a two-lobe shape).
- The displacement indicator(s) may be loose or prone to vibration.
- Finite resolution of the displacement indicator.
- Data acquisition noise and resolution.
- Number of turns included in measurements.
- Performance variations under load.
- Dependence on speed and possibly direction of rotation.
- Influence of temperature, vibration, and air supply pressure changes.
- Influence of spindle drives on the measured performance.

In the first three case studies that follow, the spindles are installed in working machine tools. For this reason, the results reflect the combined contribution of the spindle along with the entire workpiece-to-tool structural loop. While this information is not necessarily helpful in isolating spindle problems, it provides an accurate picture of the total displacement between the tool and workpiece.

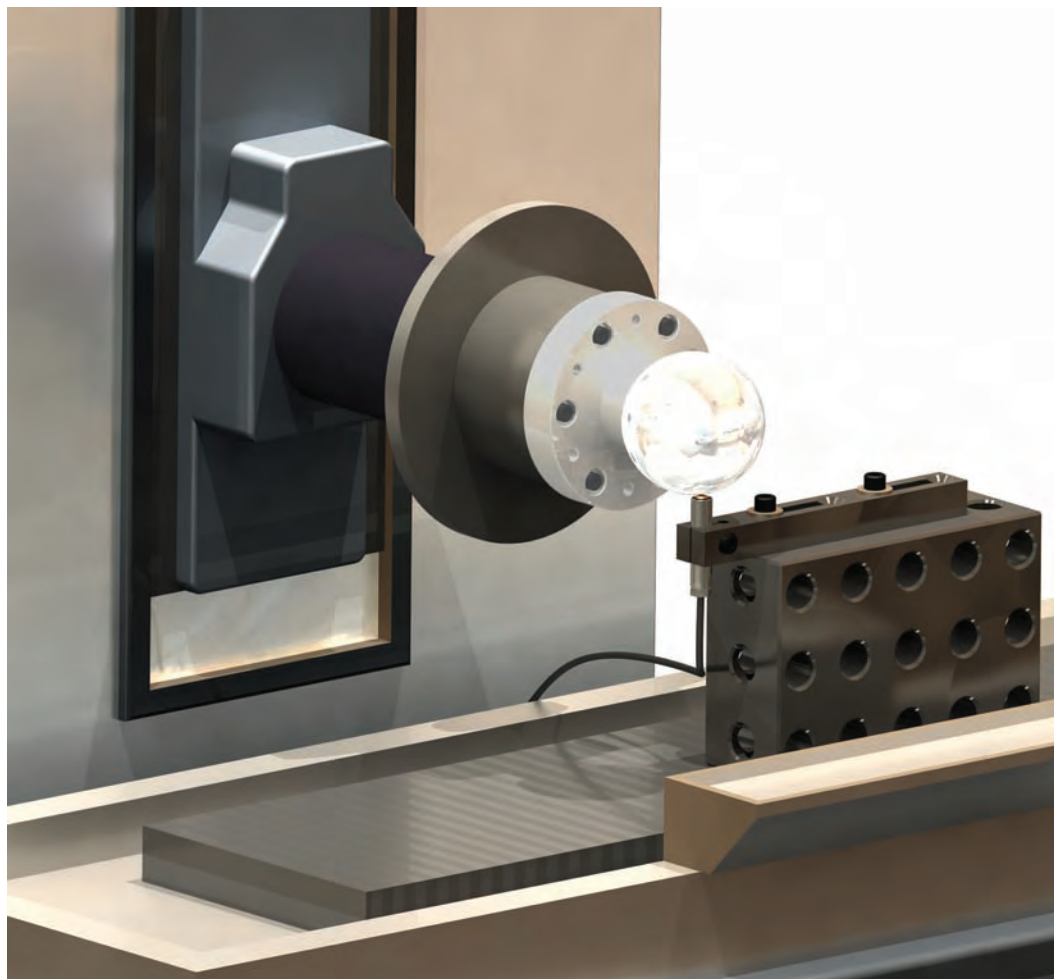


**Figure 5.1** Manual surface grinder with a ball bearing spindle. The grinding contact has a fixed sensitive direction, and only one displacement sensor is needed to capture the motion in the relevant (vertical) direction. Note that the probe is mounted with a very short overhang so that the fixturing assembly is as stiff as possible.

## 5.1 Surface grinder spindle

We begin by considering a typical, manually-operated surface grinder. The grinder has a single-speed AC motor to drive the spindle through a coupling. The test setup is straightforward because the displacement indicator fixturing can be conveniently positioned using the grinder's  $XZ$  table and locked down using its magnetic chuck. The workpiece is only sensitive to vertical motion between the chuck and grinding wheel. Because the workpiece/wheel contact is always sensitive to relative motion in the vertical direction, testing will be carried out with fixed sensitive direction calculations.

Conventional surface grinding wheels are dressed with a single point diamond at the same point as the contact between the workpiece and wheel. As discussed in Chapter Two, this will mean that the

## 5.2 Lathe spindle

The surface grinder only required one measurement for complete characterization of the relevant spindle and structural motion. We will now consider a CNC lathe, which requires additional measurements because the workpiece may be turned on the face, on the outer or inner diameter, or some combination in a contouring cut. In turning operations, the locus of points on which the tool may have contact with the workpiece falls on a fixed (i.e., non-rotating) plane. For this reason, we only need to consider our measurement as a fixed sensitive direction. Figure 5.2 shows the lathe along with a five-channel Lion Precision Spindle Error Analyzer system used to capture and analyze the data. Although only three probes are needed in this application, five are shown, because it is easy to gather the additional information.

In this example, we consider structural and spindle error of a CNC lathe while increasing the sophistication of our setup to accommodate the additional degrees of freedom. Although we only require measurements at two radial and one axial location, the results can be extrapolated to any other radial or face location.

Figure 5.2 shows the CNC machine tool with a dual-sphere artifact in the three-jaw chuck being measured by capacitive probes. Figure 5.2 shows another view of the probes and artifact. The probe fixture is a rigid bracket mounted in place of one of the cutting tools.

### Thermal response

Before looking at spindle and structural error motion, we can use the same artifact and probes to characterize the thermal response of the structure. In this example, the lathe is not running. Instead, we focus on the response of the machine to changes in the ambient air temperature. Figure 5.2 shows a complete 24-hour cycle. A few extra hours are also shown to demonstrate how the fluctuations are cyclical as a result of a fairly repetitive operation of the shop HVAC system from day to day. The response does not perfectly repeat because the outside air temperature varies, and the HVAC system load varies in response.

The thermal response plot shows that the five displacements vary by 3 to 4 micrometers during the 30-hour period. There is a significant correlation of the ambient air temperature to the other measured quantities. The temperature measured on the turret and spindle are tempered by the thermal inertia of the iron castings to which the thermistors are attached. While the air temperature spikes quickly as the HVAC system switches off and on, the machine's response is much slower.

The measured displacements span the entire structural loop from the cutting tool to the workpiece. As seen in the figure, the machine

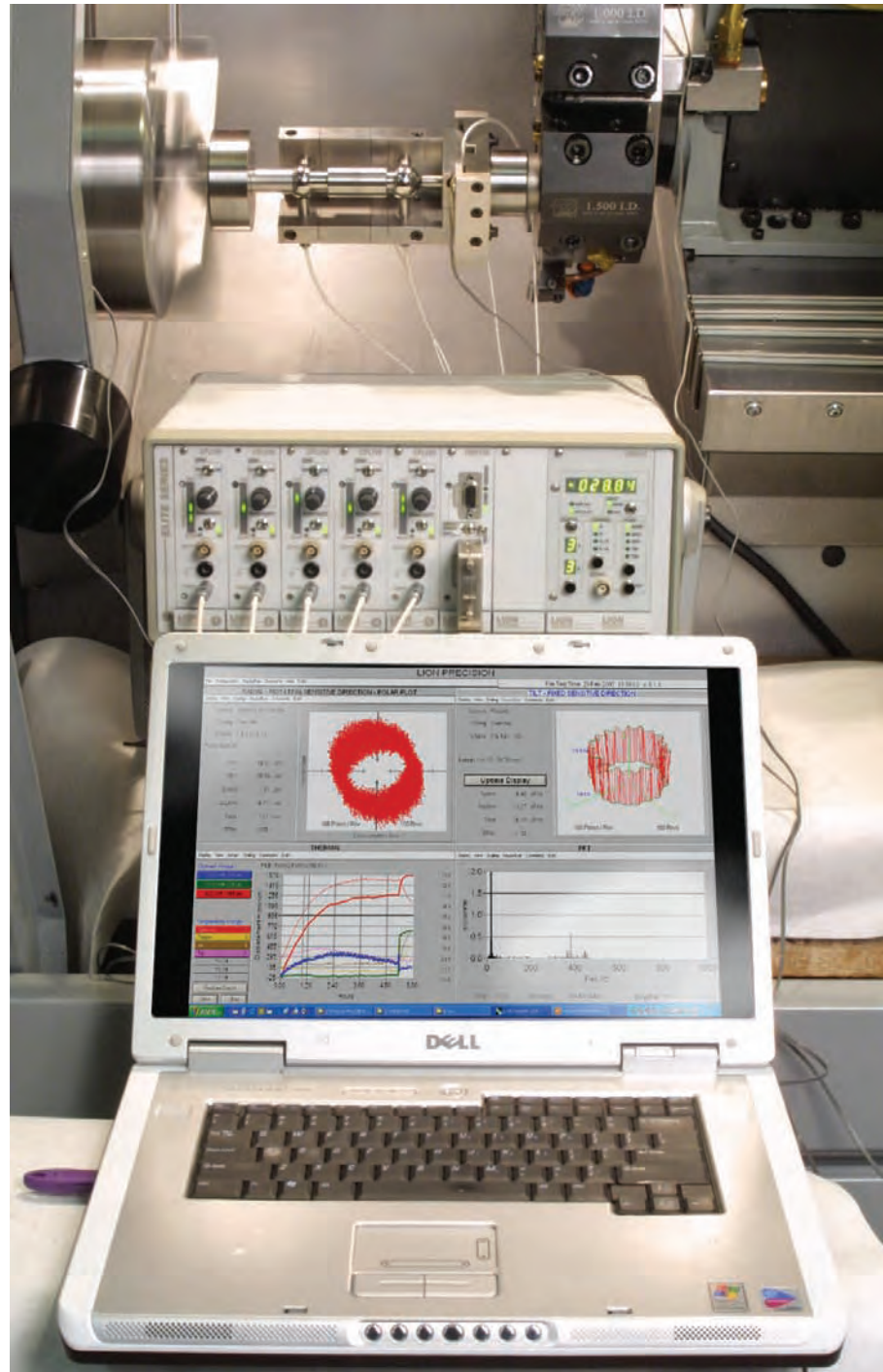


**Figure 5.6** CNC lathe with an angular contact ball bearing spindle and variable speed AC drive.. Five probes are configured for measuring motions capturing all five degrees of freedom. The probes are located in the place of the tool and will measure the combination of spindle error, structural error, and the effects of any disturbance to the machine.

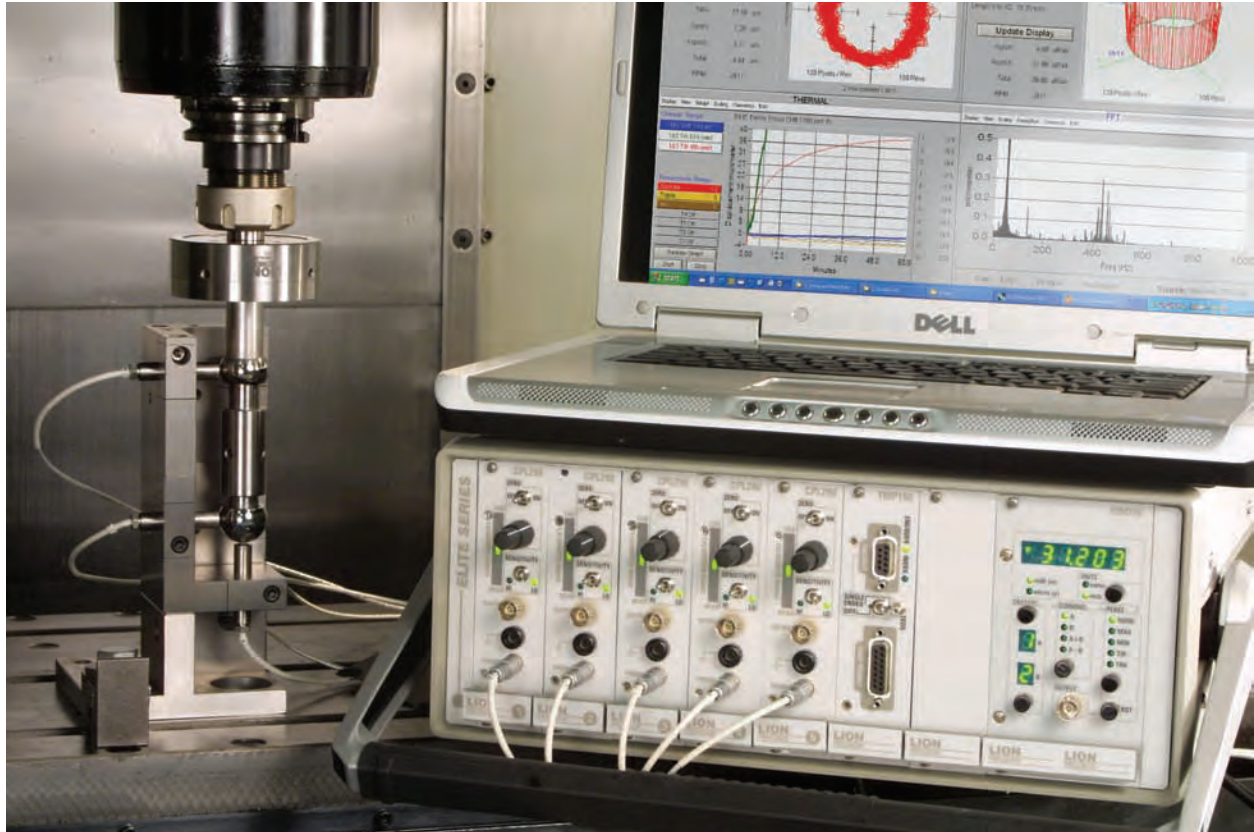


**Figure 5.11** CNC vertical machining center with variable speed, AC motor and angular contact, ball bearing spindle.. The probes are configured for measuring motions capturing all five degrees of freedom. The probes are located in the place of the tool and will measure the combination of spindle error, structural error, and the effects of any disturbances to the machine.

### 5.3 Milling machine spindle

The measurements outlined for the lathe and surface grinder are readily made on a 3-axis milling machine as well. Figure 5.3 shows the arrangement of fixturing and probes along with a dual-sphere artifact to make the measurement.

As with the lathe, the two radial measurements allow computation of the tilt component. Once the tilt is known, the synchronous error can be extrapolated for any radial or face location. However, as with most ball bearing spindles, the synchronous motion is relatively small compared to the asynchronous. In most cases, the metrologist will be particularly interested in the larger asynchronous component, in order to identify and solve problems.



**Figure 5.13** The PI 5.5 ISO is designed for maximum accuracy in a compact package. Its captured thrust between large radial bearings provides high stiffness in a spindle that can be operated at high speeds.

## 5.4 Air bearing spindle for diamond turning

This air-bearing spindle is built for ultra-precision diamond-turning lathes. The requirements include 1000 N load capacity, 6000 RPM operation, 20 nm radial error motion, and minimal thermal growth. These competing specifications are met using a captured thrust design to minimize the heat generated in the air-films. Even so, the ISO 5.5 shown in Figure 5.4 generates 125 Watts of heat at 6000 RPM, which is dissipated by cooling jackets.

The performance specifications of the spindle are so exacting that its development and production required completely new metrology tooling, which was revised over several iterations. This section reviews a few of the lessons learned while testing and will conclude with a look at plans for using error separation techniques at high speeds to reduce the last few nanometers of artifact error from the tests.

### Test stand development

It is good practice to test air bearing spindles before installing the motorization. At low speeds, test stands using conventional off-the-shelf indicator mounts give reasonable looking results, and details

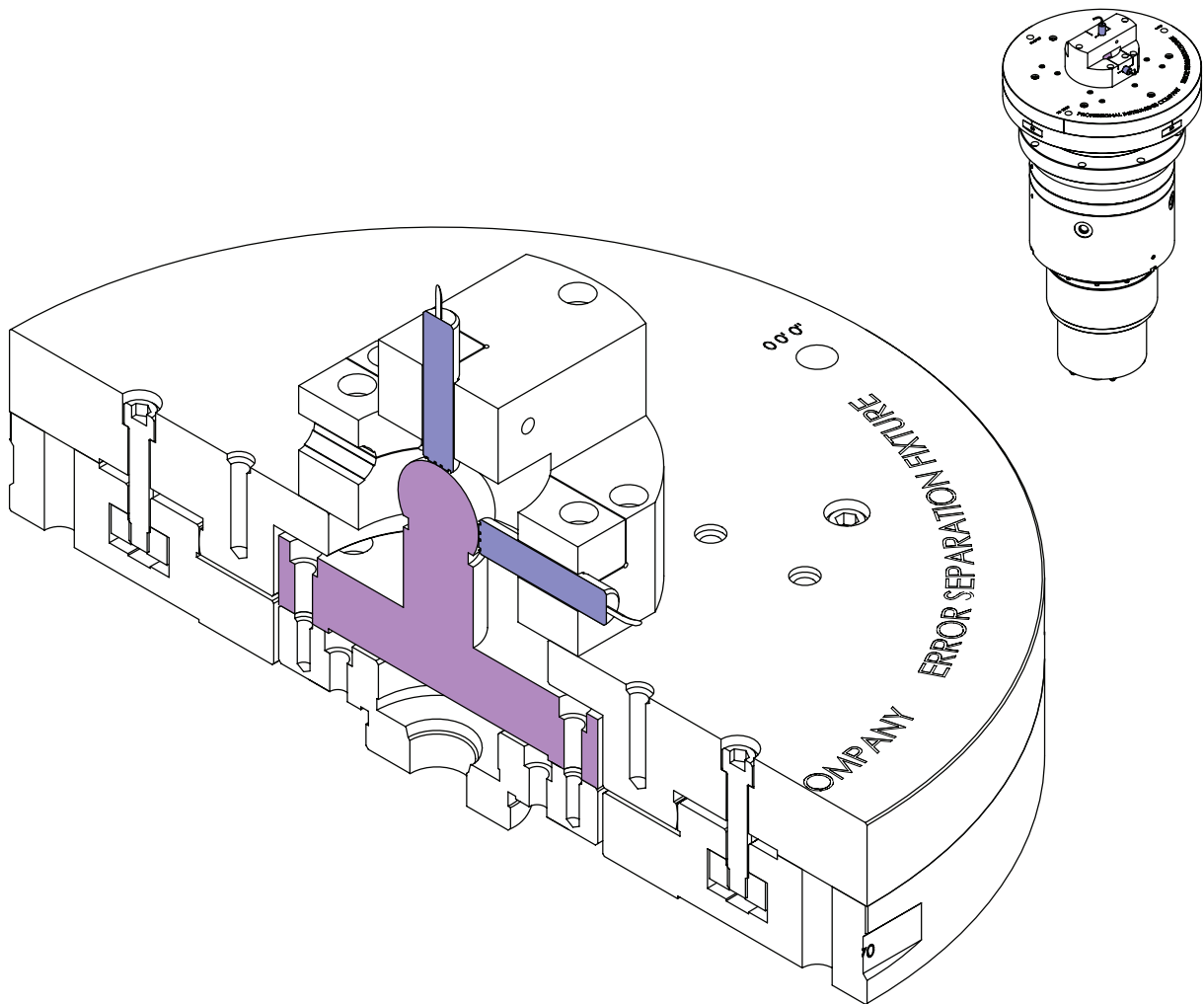


**Figure 5.18** Future concept for implementation of the multiprobe error separation method using three index points at 0, 99.844, and 202.5 degrees on the PI ISO 5.5 spindle. This allows separation of target error from spindle error at high speeds.

# Chapter 6

## Applications

### 6.1 Tapered roller bearing spindles

Roller bearing spindles offer high load capacity and stiffness because of line contact between the rollers and races. The trade-off in performance is that these bearings typically have relatively large error motions, because any geometrical errors in the rollers or races print through to the rotation by the same internal stiffness that provides the favorable load capacity.

The results that follow demonstrate the performance that can be achieved when every detail is carefully engineered and manufactured. At present, the performance limitation is the setting of the spindle preload and the accuracy of the rollers whose imperfections cause asynchronous error motion.

Figure 6.1 shows an example of axial and radial error motion measured on a PI 4RT tapered roller bearing spindle. This spindle is bolt-for-bolt compatible with the 10,000 RPM 4R BLOCK-HEAD<sup>®</sup> line of air bearing spindles with the added advantage of much higher load capacity and even higher stiffness. This spindle is rated to speeds up to 400 RPM.

### 6.2 Instrumentation for rolling element bearings

This section describes an instrument to measure the error motion of rolling element bearings by simultaneously satisfying four requirements. First, an axial preload must be applied to seat the rolling elements in the bearing races. Second, one of the races must spin. Third, rotation of the remaining race must be prevented in a way that leaves the radial, axial/face and tilt displacements free to move. Finally, the bearing under test must be fixtured and measured without introducing unintended off-axis loads or other distorting influences.

Figure 6.2 shows a dedicated instrument for measuring precision bearings. In the design presented here, an air bearing reference spin-



Test	Error motion (nm)			RMS error motion (nm)			RMS torque (mN-m)		
	Synch	Asynch	Asynch	Low	Med	High	Low	Med	High
	P-V	P-V	$4\sigma$	1.7-10	10-60	60-300	1.7-10	10-60	60-300
1	31	560	290	36	15	2	1.2	1.9	0.2
2	35	510	280	46	16	3	1.5	2.4	0.2
3	26	710	440	43	15	3	2.1	2.2	0.2
4	31	630	380	50	19	3	1.7	3.0	0.2
5	35	590	320	47	17	3	1.7	2.9	0.2
mean	32	600	340	45	16	3	1.7	2.5	0.2
$\sigma$	4	78	67	5	2	0	0.3	0.5	0.0

**Table 6.2** Repeatability results for radial error motion and torque. The low, medium, and high ranges are multiples of the input shaft speed, as reported in Anderometer-style measurements.

aging additional revolutions of data reduces the measured value for synchronous error motion and increases the apparent asynchronous value. In the results that follow, 512 revolutions were used in all computations. This number of revolutions was found to give stable results while providing sufficient frequency domain resolution within a reasonable amount of test time.

### 6.3 Rolling element bearing repeatability

Table 6.3 shows data from consecutive measurements taken on a 6204 ball bearing at 1000 RPM for 512 revolutions under 100 N of axial preload. The tabulated motion and torque values have a standard deviation of approximately 15 to 20% of the mean. In the case of the 6204 bearing, the repeatability is better than 100 nm for the overall magnitude of the radial error motion, and torque repeatability is better than 1 mN-m.

The most significant (i.e., largest) frequency component in the data tabulated in Table 6.3 occurs at the cage rotation frequency at 38.5% of the shaft rotation frequency. This component is below the range included in the three frequency bands of the Anderometer. For this reason, the low-medium-high band results, which start at 1.67 times the shaft rotation speed, do not share the same general magnitude as the asynchronous component, which includes all non-integer multiples of the shaft rotation frequency down to 0 Hz.

The instrument repeatability is also apparent in the frequency domain. Figure 6.3 shows four FFT plots of the radial error motion calculated from 512 revolutions of data sampled 1024 times per revolution. As before, the results show little variation in consecutive tests. Furthermore, the frequency components associated with particular geometric defects of the ball bearing occur at identical frequencies and similar amplitudes for all tests, as summarized in Table 6.3. The high consistency in the frequency domain data suggests that the bearing frequency components combine in somewhat

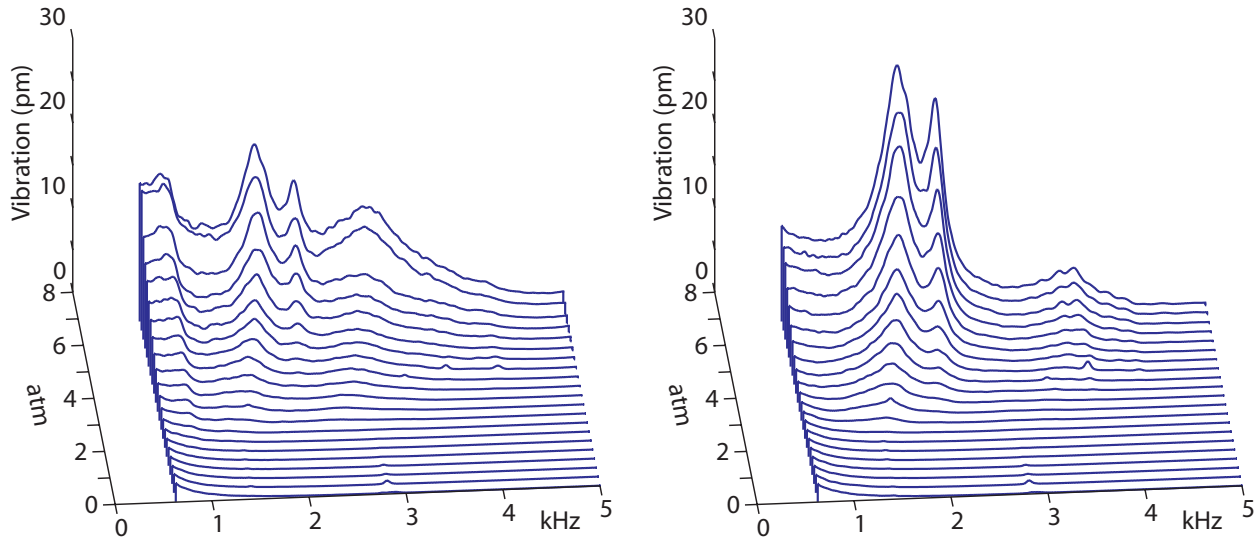


**Figure 6.9** (a) Axial and (b) radial vibration in an externally-pressurized spindle with air as the working gas. The rigid-body response at lower frequencies is large because of the compliant support and is not plotted. Note use of picometers on vertical scale.

## 6.5 Air bearing stiffness and pressure

The performance of air bearing spindles varies with the supply pressure of the working gas. This effect is demonstrated here on tests run on a PI ISO 3.25 spindle with groove compensation. The spindle used in this work is not installed in a machine, but rather rests on a compliant foam pad on an air isolation table. Temperature is controlled to  $20 \pm 1^\circ\text{C}$ , and the supply gases are drawn from cylinders. A single regulator was used to tap all gases using simple threaded adapters to accommodate the different bottle connector styles. This main regulator was left undisturbed in all testing at 10 atm. A second pressure regulator was used to adjust the pressure between 1 and 7 atm as needed. The same 2 m air line and fittings are used in all testing. A high-sensitivity triaxial accelerometer is fixed to the stationary spindle rotor face plate to measure vibration in the axial and radial directions.

Figure 6.5 shows the vibration spectra measured on the stationary spindle at different supply pressures from 0.3 to 7 atm in 0.3 atm increments. These waterfall plots are constructed from 21 separate tests of 500 averages each. At the lower supply pressures, the RMS vibration level in the frequency range of 400 to 5000 Hz is less than 1 pm. At higher air supply pressures, the RMS vibration increases monotonically to 11 pm at 7 atm. Because the individual spectral lines are obtained by twice integrating an accelerometer signal in the frequency domain by dividing by  $(2\pi f)^2$  and because the spindle floats on a compliant support during testing, the lower frequencies do not provide relevant information and are removed for clarity.

# Index

- air bearing
  - compensation, 16
  - gas viscosity, 145
  - mean free path, 146
  - pressure dependence, 140
  - stiffness, *141*
  - working gas, 142, *143*
- air film averaging, 16
- aliasing, *61*
- Arneson, Harold, 9, 37
- Arneson, Ted, 9
- artifact
  - double ball, *13*
  - eccentricity, 4
  - quality, 15, 43
- B89.3.4 Standard
  - error types, 22
  - history, 10
- balance, 6
- ball bearings
  - analysis, 134–139
  - repeatability, 139
- Bryan, James, 10
- capacitance sensor
  - contact adapter, 44
  - design, 44
  - drive crosstalk, 51
  - noise, 53
  - performance, 48
- capacitance sensors
  - physics, 44
- capacitive sensor
  - advances, 11
  - performance, 3
  - requirements, 2
  - sensitivity, 2
- case studies
  - air spindle, 121
  - CNC lathe, 113
  - error separation, 98
  - gyroscope, 9
  - milling machine, 119
  - precision lathe, 3
  - sensitive directions, 32
  - spheres, 9
  - surface grinder, 107
- data
  - clipping, *63*
  - synchronization, 42, 63
  - vector size, 25
- DC offset, 25
- Donaldson, Robert, 10
- error separation
  - discrepancy, *103*
  - Donaldson, 75, *78*
  - Estler, 77
  - Grejda reversal, 93
  - multiprobe, 81, 83
- error separation, multistep, 86
- Estler, W. Tyler, 74
- Evans, Christopher, 74
- filtering
  - analog-to-digital, 60
  - results, *71*
  - zero-phase-shift, 59
- Grejda, Robert, 33
- harmonic suppression, *84, 85*
- Hocken, Robert, 74

- Liebers, Melvin, 10
- Lion, Kurt, 46
- measurement
  - compliance, 124
  - equation, 20
  - external influences, 55
  - hardware design, 22
  - hardware setup, 107, 114, 119, 122
  - issues, 106
  - stiffness, 109
  - thermal growth, 110, 113
- Moore, Richard, 22
- Moore, Wayne, 1, 15
- NIST GUM, 98
- Nyquist frequency, 59
- reversal
  - straightedge, 15
- reversal chuck, 94, 96
- roller bearings
  - analysis, 130
  - measurement, 128, 127–134
  - performance, 128
- rotary encoders, 4
- Schlesinger, Georg, 8
- SEA analysis software, 12
- sensitive direction
  - calculation, 31
  - fixed, 28
  - rotating, 29
- sensor resolution, 42
- Sheridan, Timothy, 12, 60
- Slocum, Alexander, 1
- Smith, Philip, 49
- spindle, 1
  - high-speed, 2
  - perfect, **16**
- spindle error
  - asynchronous, 6, 25, 67
  - axial, 4, 18
  - classification, 18
  - compared to artifact, 4
  - definition, **1**
  - FFT, 7
  - fundamental, **5**, 5, 24
  - mapping to workpiece, 3, 21, 22, 28
  - separation, 16
  - synchronous, **6**, 6, 24, 67
  - tilt, 20
  - troubleshooting, 7, 24
  - visualization, 73, 74
  - vs. runout, 8, 100
  - vs. structural error, 43
- thermal compensation, 23
- thermal growth, 8, 56
- Thusty, George, 6, 9
- triggering, 4
- uncertainty, 98
- Vallance, R. Ryan, 49